Cloning and Characterization of Protein Fraction Specific of Chlorella vulgaris Endemic East Java

Yanuhar, Uun
Departement of Aquatic Resource Management, Faculty of Fisheries and Marine Science, Universitas Brawijaya

Suryanto, Heru
Center of Excellence for Cellulose Composite (CECCom), Department of Mechanical Engineering, Faculty of Engineering, Universitas Negeri Malang

Mahasri, Gunanti
Faculty of Fisheries and Marine, Airlangga University

Nico Rahman Caesar
Environmental Science, Postgraduate Programme, Universitas Brawijaya : Doctoral Programme

https://doi.org/10.5109/7172229

出版情報：Evergreen. 11 (1), pp.82-94, 2024-03. 九州大学グリーンテクノロジー研究教育センター
バージョン：

Cloning and Characterization of Protein Fraction Specific of *Chlorella vulgaris* Endemic East Java

Uun Yanuhar[1*], Heru Suryanto[2], Gunanti Mahasri[3], Nico Rahman Caesar[4]

[1]Departement of Aquatic Resource Management, Faculty of Fisheries and Marine Science, Universitas Brawijaya, Jl. Veteran Malang 65145, East Java, Indonesia

[2]Center of Excellence for Cellulose Composite (CECCom), Department of Mechanical Engineering, Faculty of Engineering, Universitas Negeri Malang, Jl. Semarang 5, Malang 65141, Indonesia

[3]Faculty of Fisheries and Marine, Airlangga University, Jl. Airlangga No.4, Surabaya 60115, East Java, Indonesia

[4]Doctoral Programme of Environmental Science, Postgraduate Programme, Universitas Brawijaya. Jl. MT Haryono No.169, 65145 Malang, East Java, Indonesia

E-mail: doktoruun@ub.ac.id

(Received March 23, 2023: Revised January 13, 2024: Accepted January 14, 2024).

Abstract: *Chlorella vulgaris* is a type of microalgae that contains active chemical metabolites, including Pigment-Protein Fraction (PPF), which has been shown to possess anti-viral and anti-inflammatory properties in fish viral infections. The objective of this study is to characterize PPF of *C. vulgaris* through cloning and in silico analysis. This study utilized *C. vulgaris* isolated from the endemic region of East Java, Indonesia. The morphology of the cultured microalgae was observed using a scanning electron microscope (SEM). The PPF was characterized using the SDS-PAGE method, and its cDNA was isolated and analyzed through RT-PCR. Subsequently, the gene was cloned, transformed using *E. coli* DH5α, and sequenced. The structure and function of PPF were then described through an in-silico procedure. The study revealed that the cultures of *C. vulgaris* had a high cell density, with a density of 772 x 10^4 cells/mL after being cultured for 7-8 days. The morphology of the microalgae was observed to have a smooth surface with a diameter ranging from 1.5 µm to 2.67 µm. The PPF had a molecular weight of 14 and 35 kDa and its cDNA was visualized using RT-PCR, which revealed a protein with an alkaline pair length of 313 bp. In silico analysis identified two compounds in PPF of *C. vulgaris*, namely, *Succinate CoA ligase* and *Ammonia form cytochrome c nitrite reductase*. These compounds were found to have functions such as protein kinase activity, catalytic activity, and regulation of gene expression.

Keywords: capsid protein; cloning; *C. vulgaris*; PPF; protein structure.

1. Introduction

Microalgae are known to be one of the largest producers of proteins and active chemical metabolites in the aquatic environment[1]. These compounds have been found to have anti-bacterial, anti-viral, and anti-fungal properties, which can be effective in preventing biofouling and other issues. In addition, biogenic compounds from algae have potential uses in therapy[2,3]. Marine algae, including brown algae, green algae, and red algae, are promising sources of natural bioactive compounds and proteins with potential applications in the pharmaceutical industry. These bioactive compounds and proteins have been found to have a wide range of properties and potential uses, including anti-tumor, anti-bacterial, and anti-cancer effects, among others[4]. There is growing interest in studying and exploiting marine algae as a source of bioactive compounds and proteins, potentially benefiting human and animal health[5,6].

Microalgae have significant potential as an alternative source of protein and bioactive ingredients for the health of fish and shrimp, particularly in aquaculture systems. Natural feed is essential for the early stages of the development of aquatic organisms, and microalgae can provide a high-quality, renewable source of nutrition for fish and shrimp and a source of energy[7,8]. *C. vulgaris* is amicroalgae with various potential substances: proteins, vitamins, minerals, carbohydrates, fats, chlorophyll, *beta-carotene*, cellulose 15.4%, hemicellulose 31%, glucosamine 3.3%, and ash containing a lot of iron and lime[9)4], and also the Protein Pigment Fraction (PPF), which is part of the protein[10].

Protein pigments are nutrients in microalgae and generally produce pigments that can absorb sunlight energy in photosynthesis[11,12]. According to some studies, the pigment fragment of the protein pigment *Chlorella* has numerous benefits. It has the potential to be developed and used as an anti-viral and anti-inflammatory agent in viral infections of grouper fish[13,14]. Previously, Yanuhar *et al.* (2020) investigated the effects of *C. vulgaris* administration on *β-actin* and MHC-1 responses in groupers infected with *Viral Nervous Necrosis* (VNN). The augmentation of PPF resulted in an upsurge in the expression of MHC-1 and *β-actin*, indicating a strengthened immune response in *C. altivelis*. This, in turn, reduced the harm inflicted on the eye tissue of fish infected with VNN[10].

An In silico approach using molecular docking mechanisms is one of the keys in molecular biology to determine the structure of functions and design drugs with the help of computerization. The specific purpose of characterizing it structurally with the Silico technique of a bond-protein docking bond is to predict the dominant binding mode of the ligand with proteins with a three-dimensional structure[15,16]. This mechanism can predict molecular interactions between proteins, protein properties, biological process predictions, molecular function predictions, and cellular component predictions[17]. Characterizing PPF and its interaction with the VNN virus capsid can provide insights into the potential use of PPF as an anti-viral agent. By predicting the molecular interactions between PPF and the virus capsid, researchers can obtain valuable information on how PPF can inhibit the replication of the virus and prevent its spread. Given the high potential use of PPF, this study aims to determine the character of PPF from the isolation of *C. vulgaris* and predict the model of its interaction with the VNN virus capsid. This can pave the way for developing new anti-viral drugs based on PPF that can be used to treat viral infections in fish and other aquatic organisms.

2. Materials and Methods

2.1 Sample of *C. vulgaris*

C. vulgaris samples result from local isolated cultures from Situbondo waters and were propagated at the Situbondo Brackish Water Aquaculture Fisheries Center (BPBAP), East Java Province, Indonesia. The *C. vulgaris* microalgae used have been molecularly identified previously and showed that the samples used show *C. vulgaris* species[18].

2.2 *C. vulgaris* Culture Endemic to East Java Waters

C. vulgaris culture was carried out in laboratory-scale cultures (agar culture, test tube, and Erlenmeyer). The culture begins with sterilizing the medium with 10 ppm chlorine and neutralizing it with 5 ppm thiosulfate. After neutralization, the Walne fertilizer was applied at a dose of 1 mL/liter (PA), the seedling-to-media ratio was 3:7, the temperature was kept at 25 ºC, and irradiation was done with TL lamps 40 watts 2 pieces for 5-7 days. Overnight (1 day) culture on nutrient agar media (NA), then transfer colonies from medium nutrient agar into a 10 mL test tube containing TSB (*Tripton Soya Broth*). After the microalgae cells have grown, place them in 100-200 mL Erlenmeyer culture medium for 3-4 days. A pure culture was propagated in 1-liter culture and later in Erlenmeyer 5 L. During the culture period, the growth of *C. vulgaris* was observed, and its density was calculated using Eq. (1)[13]:

$$Number\ of\ Cells = \frac{\text{Total number of cells}}{\text{Count Number of Cells}}\ x\ 16\ x\ 10^4 \ldots (1)$$

2.3 Morphological Observations of *C. vulgaris* using Scanning Electron Microscopy

Collected *C. vulgaris* was dried and dehydrated with ethanol concentrations, gradually increasing to 96% for 24 hours. It was transferred to *dimethyl acetal formaldehyde* for 2 hours. The sample was dried at a critical point using CO_2 on HCP: 2 Critical Point Dryer (Hitachi, Japan), then coated with a gold layer using the IB-2 ion coater, and the morphology of microalgae was observed under SEM (Hitachi S-530, Japan) at 15 KV[19,20]

2.4 Pigment-Protein Fraction (PPF) Isolation and SDS PAGE

Isolation of PPF from isolating *C. vulgaris* was carried out according to a previously published method[10]. *C. vulgaris* was harvested with a wet weight of 50 g, then homogenized for 1 hour using sterile mortar after adding liquid nitrogen to help soften the cell walls of *C. vulgaris.* Microalgae cells continued to be homogenized for 30 to 60 min. 8 mL 20 mM KCl (Sigma-Aldrich, Germany), pH 7.5, and 50 mM glycine (Merck) was added to the homogenized mixture. Next, it was centrifuged at 17000 × g, 4°C for 60 min. Supernatants were collected in a sterile Eppendorf tube. A saturated solution of ammonium sulfate (100% sat., Sigma-Aldrich, Germany) was gradually added to the supernatant until it reaches a saturation concentration of 30%. This solution was re-centrifuged at 15000 × g for 30 min at 4 °C, and then we get a supernatant. Furthermore, the supernatant was dialyzed to obtain a pure PPF protein solution supernatant. Before use, dialysis tubes were sterilized for 10 min by boiling them in a *Tris-ethylenediaminetetraacetate* (TRIS-EDTA) (Sigma-Aldrich, Germany) with a concentration of 0.1 mM and a pH of 7.3. Supernatant samples were dialyzed in 2 L of Tris-HCl solution (Sigma-Aldrich, Germany) at 4°C for 24 hours with a magnetic stirrer inside the Erlenmeyer, where dialysis was performed. After overnight dialysis, a solution in a dialysis pouch was taken, and the sample solution was filtered through a 0.22 m sartorius filter. Dialysis was done twice using the same method. A spectrophotometer was used to determine the protein content of the solution after the second dialysis.

2.5 Silver Nitrate Staining

Silver nitrate (silver stain) staining kit (Thermo Fisher Scientific Inc., USA) is used to stain the gel by first soaking it in a fixation solution (30 min) and then in a sensitizing solution (30 min). The gel was then washed by soaking it in distilled water (5 min, repeated 3 times). The gel was soaked in a silver reagent, after which it was washed in distilled water (2 min). The gel was then washed by soaking it in a developing solution (30 seconds - 5 min). Soaking should be stopped immediately when the gel turns dark by soaking it in a stopping solution (10 min). The gel was washed and soaked in distilled water (5 min, repeated 3 times). The gel was soaked in a preservative solution (30 min, repeated 2 times).

2.6 Total Protein Analysis

C. vulgaris dry powder was used as the sample. The protein content test was carried out according to the Association of official analytical chemists[21)] by taking as much as 1 g of K_2SO_4, 40 mL of HgO, and 2 mL of concentrated H_2SO_4 added to 0.5 - 1 g of sample. The sample should then be boiled for 2 hours until the liquid is clear and greenish. They poured the sample into a distillation device and a Kjeldahl flask which they rinsed with 1 - 2 mL of distilled water (3 times). Add 8 - 10 mL of 60% NaOH solution and 5% $Na_2S_2O_3$ solution to the sample. Erlenmeyer was filled with 5 mL of H_3BO_3 solution, and a BCG-MR indicator (a mixture of bromocresol green and methyl red) was placed beneath the condenser. Dedistilled the sample until 10 - 15 mL of distillate was obtained, then diluted it to 50 mL. Titrate the sample solution with 0.02 N HCl until it turns pink. Then, complete the blank assignment. The determination of N and protein levels was carried out using the Eq. (2):

$$\text{Up to N (\%)} = \frac{ml\ HCl - ml\ Blanko\ x\ N\ x\ 14.007\ x\ 100}{\text{mg sampel}} \quad ...(2)$$

2.7 Fat content analysis

The total lipid content of the sample was analyzed using the *Soxhlet* method described in Ardiansyah *et al.*[22)]. Initially, a fat pumpkin of appropriate size was prepared, dried in an oven, cooled in a desiccator, and weighed. Then, 5 grams of dried *C. vulgaris* sample was placed in a lead filter of appropriate size and covered with fat-free cotton. The lead or filter paper, containing the sample, was inserted into the *Soxhlet* extraction apparatus, and a condenser was placed on top with a fat flask underneath. The appropriate amount of diethyl or petroleum ether solvent was added to the fat flask, depending on the size of the *Soxhlet* device used. The mixture was then refluxed for at least 5 hours or until the solvent began to drip back into the fat flask. The solvent present in the fat flask was then distilled and collected.

Furthermore, the fat squash containing the extracted fat was heated in the oven (105°C). Drying was carried out until the weight remained and cooled in a desiccator, weighing the pumpkin and the fat. The weight of fat was calculated using Eq. (3):

Total fat conversion =

$$\frac{Result\ of\ the\ Total\ Fat\ Test/100}{Sample\ Weight\ and\ Total\ Density}\ x\ \frac{Fertilizer\ Dose}{1000} \quad ..(3)$$

2.8 Pigment-Protein Fraction (PPF) Characterization

2.8.1 Methods of RNA Isolation of *C. vulgaris*

The sample used for RNA isolation was a fresh paste of cultured *C. vulgaris.* Pigment-Protein Fraction (PPF) RNA isolation was carried out using purified RNA reagents and mini kit-Plant RNA (Geneaid Biotech Ltd., Taiwan). The insulation stages include mechanical cell wall damage (lysis) using mortar and pestle in a liquid nitrogen solution in a mortar dish. Liquid nitrogen was applied to help make dry tissues and cells soften and brittle, thus making them more accessible for cells to destroy. Furthermore, RNA binding, RNA leaching, and RNA purification were carried out using cold methanol after incubating overnight[10)]. RNA isolation methods were according to the manufactory instructions (Geneaid Biotech Ltd., Taiwan).

2.8.2 cDNA synthesis

The procedure for cDNA synthesis was carried out according to the instructions provided by Agilent, USA for the AffinityScript cDNA Synthesis Kit. To prepare the first-strand cDNA synthesis reaction, A volume of total RNA or poly(A)+ mRNA within a range of 1 ng to 5 µg and 1 ng to 250 ng respectively, was mixed with 15.7 µl of RNase-free water and either 1.0 ul of oligo(dT) primer (0.5 ug/ µl), 3 µl of random primers (0.1 µg/ µl), or 1 µl of a gene-specific primer (100 ng/µl) in a microcentrifuge tube. The mixture was then incubated at 65°C for 5 minutes and cooled down to room temperature for around 10 minutes. To complete the reaction, 2.0µl of 10 Affinity Script RT Buffer, 0.8 µl of dNTP mix (25 mM per dNTP), 0.5µl of RNase Block Ribonuclease Inhibitor (40 U/µl), and 1µl of AffinityScript Multiple Temperature RT were added to make the final reaction volume 20µl. Before placing the tube in a thermal block with a temperature range of 42 to 55 °C, gently stir the reaction components. Incubate the reaction for 60 min. After 15 min of incubation at 70°C, put an end to the reaction. Put the finished first-strand cDNA synthesis reactions on ice to be amplified by PCR.

2.8.3 RT PCR assay of the PFF gene from cDNA 313 bp. *C. vulgaris*

Amplification aims to multiply cDNA fragments from the RT-PCR process with a specific primer. The components required in one PCR reaction were 12.5 µl Go taq green, 8.5 µl ddH2O, 1 µl Primer F 10 mM, 1 µl Primer R 10 mM, and 2 µl cDNA. The total amount of reagents used in one PCR reaction was 25 µl. Peridinin-Chlorophyll-Protein (PCP) primers (Table 1.) were used in cDNA amplification following the procedure[10,23]. Amplification with PCR was performed 35 times with predenaturation, denaturation, annealing, and elongation. The predenaturation stage was carried out at 94ºC for 5 min and the denaturation stage was carried out at 94ºC for 1 min. The annealing stage was carried out at 50ºC for 1 min, where the forward primer and reverse primer were attached to a single strand of DNA in each complement. The final elongation synthesis occurred at 72ºC for 5 min and 40ºC for storage temperature.

Table 1. The specific primer used RT-PCR[23].

Specific primers	Primary arrangement	Target gene (bp)
Initial primer	5'-GCATGAAGCCACTTCGAAAC-3'	310-316
RNA Adapter	5' – CTCGTTGCTGGCTTTGATG – 3'	
Nested primer	5'-TAACGCTGGGATGCTTTGAC-3'	

2.9 Cloning and Gen Transformation of PPF *C. vulgaris*

The cDNA isolated from *C. vulgaris* was transformed into E. coli using the pTA2 Vector and the Target Clone Plus Kit. The PPF gene was transformed using Mix and Go Competent Cells™ with *E. coli* Strain Zymo 5α (Zymo Research). The next step involved isolating plasmid DNA from the *E. coli* carrier of the PPF target gene, which was carried out following the protocol of the ZR Plasmid Miniprep Kit (Zymo Research). To confirm the insertion of the PCP gene, PCR was performed using the primary promoters T3 and T7 with KOD FX Neo (Toyobo). The cloning results were then stored in stock glycerol for further propagation if needed. The PCR results of positive colonies containing the inserted gene were then sequenced[10].

2.10 Sequencing Gene of PPF *C.vulgaris*

Once the PPF gene encoding sequence had been identified, the gene was amplified from genomic DNA using *BigDye® Terminator v3.1 Cycle Sequencing Kit Applied Biosystems* (Applied Biosystem, USA) to obtain its nucleotide sequences.

2.11 In silico analysis of PPF *C. vulgaris*

To carry out DNA translation to protein, the *ORF* (*Open Reading Frame*) sequence must be checked. Therefore, input was submitted to the NCBI *ORF* Finder (https://www.ncbi.nlm.nih.gov/orffinder/) which identified several *ORFs* along with the translated protein sequence. The DNA nucleotide sequence obtained as a result of RT PCR amplification of PPF from *C. vulgaris* was validated using an in silico method. This method involves inputting the sequencing results to the *BLASTn* tool on NCBI, and confirming DNA similarity by examining the query cover and percent identity. To check for the similarity of translated proteins, the *BLASTp* tool on NCBI was used. The highest query cover and percent identity generated by *BLASTp* were recorded and analyzed, similar to *BLASTn*.

After obtaining the protein sequence, de novo protein modeling was performed using *I-TASSER* (https://zhanggroup.org/I-TASSER/). The protein was then characterized using PSI-blast-based secondary structure PREDiction (*PSIPRED*) tools and Discovery Studio R17 software. The protein targets for receptor samples were obtained from the PDB database (ID 4RFU), specifically the Crystal structure of truncated P-domain from *Grouper nervous necrosis virus* capsid protein at 1.2A. The *Succinate CoA ligase*, which was previously modeled using *I-TASSER*, was used as the ligand.

Two docking methods were used to determine molecular interactions between proteins: (1) blind docking using the *ClusPro* web server as a representative of rigid docking tools, and (2) flexible docking using the Haddock web server as a representative of flexible docking tools. The amino acid interactions were further visualized using Ligplot.

3. RESULTS AND DISCUSSION

3.1 Culture of *C. vulgaris*

The density calculation results of *C. vulgaris* showed a gradual increase in cell density during the initial growth phase (Table **2**). The culture density reached 728 x 10^4 cells/mL after 8 days of growth. Subsequently, a larger-scale culture of 20 L was conducted for 8 days, which resulted in a density of 772 x 10^4 cells/mL. The microalgae cells were observed to adapt to the new environmental conditions[24,25]. Mass culture yields are obtained after the algae growth phase begins, which is typically from days 0-3 and is named the lag phase. From day 4 to day 7, it is expected to enter the exponential phase (peak period), during which the development of *C. vulgaris* cells experiences peak growth. Days 8-10 are typically a phase of algae death, during which there is a decrease in the number of microalgae populations

Table 2. The result of calculating the density of the culture of *C. vulgaris*.

Culture day	Density (10^4 Cells/mL)	
	Erlenmeyer 5 L	Carboy 20 L
1	260	264
2	332	324
3	396	472
4	416	520
5	552	644
6	628	684
7	696	756
8	728	772

In Erlenmeyer cultures of 5 L and carboys of 20 L, the growth phase of *C. vulgaris* microalgae consists of the lag phase (adaptation), the logarithmic phase (exponential), and the stationary phase (death). The lag (adaptation) period lasts from day 0 to day 3 (Table **2**). During this period, environmental adjustments are still being made and the number of cells increases gradually, while nutrients have not been extensively used by *C. vulgaris* microalgae for growth. The logarithmic (exponential) phase lasts from the fourth to the eighth day of observation, due to a constant increase in the number of cells with high nutrient content during this phase. The stationary phase in *C. vulgaris* cultures occurs on days 9 and 10 when cell densities begin to decrease. A good harvesting age can be determined based on the growth pattern of the microalgae. Harvesting is usually done on days 5-8 when the microalgae reach their population peak or the final exponential phase[7,26]. Furthermore, the growth reaction can be affected by various factors, including the light intensity and nutrients available in the media. The optimal light intensity for the growth of *C. vulgaris* is typically between 3,000-5,000 lux, and a 40-watt TL lamp is often used. In terms of nutrients, The Walne fertilizer is recognized as the optimal medium for fostering growth patterns[27]. Following Erlenmeyer's culture, *Chlorella* was transferred into a carboy (20 L) to obtain a larger volume with the same culture treatment.

3.2 Morphology of *C. vulgaris*

In general, the structure of dry microalgae is nearly identical in that it is shaped like a sphere with a smooth surface and no micropores forming on its surface (Fig. 1). Cells of *C. vulgaris* microalgae range in size from 1.5 to 2.67 µm, which is consistent with the findings of Sukoyo *et al.* [28], who reported that *Chlorella* has an oblong-round cell shape with a midline size of 2-8 µm.

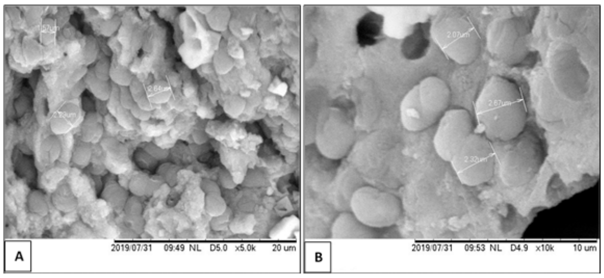

Fig. 1. Observation of the structure of *C. vulgaris* using SEM. **A.** Magnification 5000x; **B.** Magnification 10000x.

3.3 Protein Analysis of *Pigment-Protein Fraction* (PPF)

Figure 2 shows the results of the protein analysis of *C. vulgaris* using SDS-PAGE (*Sodium Dodecyl Sulfate Polyacrylamide Gel*). Protein analysis of PPF in *C. vulgaris* demonstrated that it consists of proteins weighing 35 and 14 kDa. The PPF protein has two pyridines, one in the form of a monomer (long form) with a molecular weight of 35 kDa, and the other in the form of a homodimer (short form) with a molecular weight of 14 kDa. Weis *et al.*, [23] reported that Peridinin has a molecular weight range of 14-16 kDa for monomers and 30-35 kDa for dimers. Other researchers found that homodimer peridinin has a monomer molecular weight of 15 kDa and a dimer molecular weight range of 32-35 kDa[10,14,29].

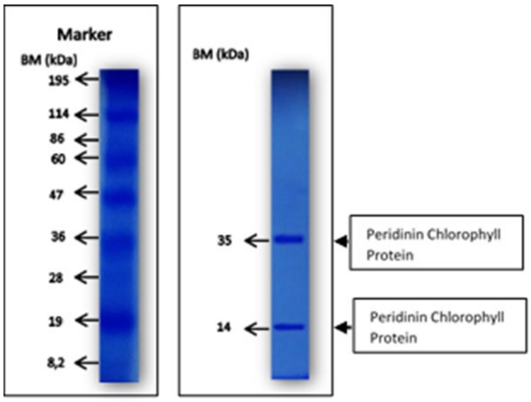

Fig. 2. PPF protein profile results in *C. vulgaris* microalgae.

The profile of the PPF protein is more clearly visible when stained with silver nitrate (silver staining). Figure 3 shows the results of the visualization of the PPF protein in *C. vulgaris* after confirmation with SDS-Page and silver staining.

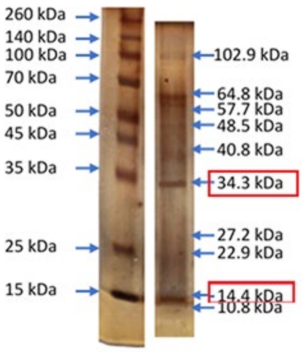

Fig. 3. PFF protein profile of *C. vulgaris* using silver staining. (A) Marker (PRO-STAIN TM), (B) Electrophoresis results of *C. vulgaris* crude protein band with SDS-PAGE.

Some PPF protein analyses are known to act as inducers, activating specific genes involved in protein expression, including *β-actin*, which functions in the immune system of fish, such as grouper (*C. altivelis*), to combat *Viral Nervous Necrosis* infection[10]. The effect of this inducer is highly dependent on the target cell's receptors, which recognize the inducer as a protein molecule[30].

3.4 Total Protein and Fat Analysis of *C. vulgaris*

The total protein and fat content of *C. vulgaris* microalgae was determined using visualization analysis standards through Uv-vis spectrophotometry at 260 nm (Table 3). Based on the protein and fat content in milligrams per cell of each microalgae, the culture treatment was repeated in the K1, K2, and K3 treatments.

The total protein content was obtained in the range of 2.19 - 4.02 x 10^{-13} (mg/cell) (culture code K2-K1), and the total fat content of Chlorella was in the range of 3.62 – 4.98 x 10^{-09} (mg/cell) (code K2-K3). The protein and fat content varies depending on the number of microalgae cells counted and the amount of biomass added to the culture. During the stationary phase, the photoperiod's influence increases the lipid and protein content of microalgae while decreasing the formation or synthesis of *n-3 polyunsaturated fatty acids* (PUFA)[31)]. The microalgae predominantly contained saturated fatty acids, with *n-hexadecanoic acid* comprising 39.7%, followed by *tetradecanoic acid* at 14.88%, and *hexadecanoic acid*, *15-methyl-*, and *methyl esters* at 11.12%[32,33)]. Polyunsaturated fatty acids, such as octadecanoic acid, constituted the second-highest proportion, accounting for 15.63% of the total. Furthermore, a small amount of monounsaturated fatty acids, specifically 2.47% oleic acid[34)] was also present. In general, algae species will synthesize large amounts of lipids stored in chloroplasts, such as TAG (*triacylglycerol*), as a form of response to adverse environmental conditions[35)].

Table 3. The total protein and fat content of *C. vulgaris*.

Treatment	Proteins of each cell (mg/cell)	Fat per cell (mg/cell)
K1	4.02 x 10^{-13}	4.47 x 10^{-09}
K2	2.19 x 10^{-13}	3.62 x 10^{-09}
K3	2.45 x 10^{-13}	4.98 x 10^{-09}

3.5 Cloning and Characterization of PPF *C. vulgaris*

Fresh *C. vulgaris* microalgae isolate (Fig. 4) were washed with a washing buffer containing ddH_2O before being used for DNA genome analysis to obtain cDNA using RT-PCR techniques. RT-PCR was used to obtain the target complementary DNA (cDNA) of PPF *C. vulgaris* using a specific primer designed for the PPF *C. vulgaris* gene. The preliminary design was carried out by referring to the 313bp cDNA data from the PPF gene in the GenBank database.

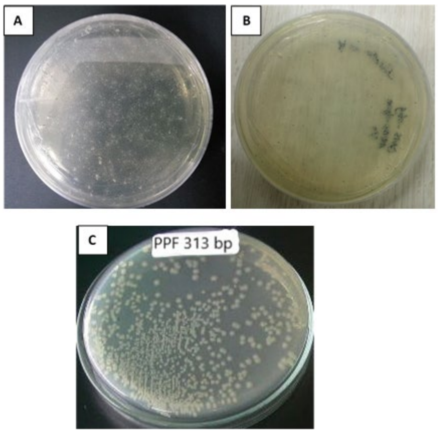

Fig. 4. PPF gene cloning in *E.coli* DH5α using Luria Bertani Broth media. (A). Top view; (B). Rearview; (C) *E. coli* colonies grew with inserted PFF313 bp gene.

Figure 5 depicts the results of the target amplification of the 313-bp-long cDNA gene of PPF *C. vulgaris*.

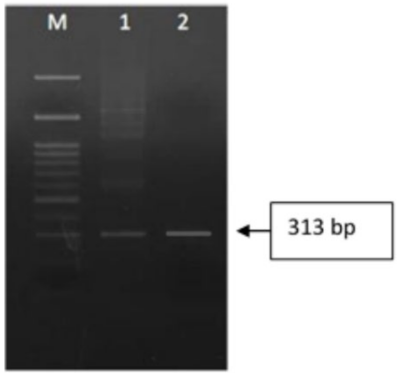

Fig. 5. The results of amplifying the PPF 310 bp gene using specific primers. M: Marker; (1) RT-PCR nested results; (2) Nested RT-PCR results after purification.

After the translation process, the cDNA of PPF *C. vulgaris*, which is the complementary DNA of the genome transcription process, forms the PPF protein. The PPF protein found in *C. vulgaris* is frequently employed as a reference for examining the interactions between pigments and pigment proteins. During photosynthesis, the PPF protein plays a crucial role in the molecular processes of absorbing light, converting it, and transferring excitation energy[36)].

3.6 Sequencing gen PPF from *C. vulgaris*

The results of the amplification of RT-PCR cDNA PPF 310 bp *C. vulgaris* and the PPF gene identification sequences from *C. vulgaris* have been successfully performed. The results of the PPF gene sequence are known to have a sequence length of 313 bp (Fig. 6.). This identification uses 3 kinds of PCP primers[23)] which have been modified in their use.

Fig. 6. PPF 313 bp gene sequence results.

Pigment-Protein Fraction (PPF) is the primary pigment involved in light harvesting or photosynthesis and is abundant in microalgae. Previous studies have found PPF in many dinoflagellate species, but research on PPF in *C. vulgaris* has been scarce. The results of this study show that *C. vulgaris* also possesses PPF, as evidenced by the successful sequencing of the PPF gene.

The results of comparing PPF gene sequences found in this study with those available in GenBank showed no similarity. This is likely due to the lack of previous studies demonstrating the presence of PPF in *C. vulgaris*. This is supported by Supasri *et al*.[37)] who showed that the length, pigment content, sequence, and spectroscopic properties of PPF can vary among different dinoflagellate groups or even among individuals of dinoflagellates.

Using the *Neighbour Joining* (NJ) method with a 1000x bootstrap, the PPF sequence of *C. vulgaris* was compared with the existing sequence data on GenBank to reconstruct a phylogenetic tree (Appendix 1). The PPF sequence of *C. vulgaris* exhibits a branching value of 54, forming a distinct branch, suggesting the occurrence of mutations or a considerable genetic distance from those previously reported in other species. This suggests that the PPF isolated from *C. vulgaris* has its own uniqueness and specific population. Phylogenetic trees describe the evolutionary lineage of a species or organism from a common ancestor. Genetic relationships between species within a population and between populations can be inferred from the phylogenetic tree created. Phylogeny is a valuable tool in comprehending the diversity of life, aiding in structural classification and gaining knowledge about the events that took place throughout the course of evolution[18,38)].

3.7 Physicochemical Characteristics of PPF *C. vulgaris*

There are 2 compounds or proteins contained in PPF, namely *Succinate CoA ligase* and *Ammonia form cytochrome c nitrite reductase* (Fig. 7 and Table 4). From the similarity test results, each compound has a different similarity value, namely *Succinate CoA ligase* with a value of 85.23%, query covers 95%, and *Ammonia form cytochrome c nitrite reductase* with a value of 68.75%, query covers 44%. Microalgae generally involves pyruvate metabolism into various reduced fermentation end products secreted from cells, e.g., formate, acetate, lactate, succinate, glycerol, ethanol, and H_2 [39)]. In the research of Atteia *et al.*[40)], conducted research and found that microalgae possess metabolic pathways for generating ATP, which helps them survive in anaerobic conditions. *Chlorella*, specifically, has a gene that encodes for a potential acetate enzyme called *Succinate-CoA* transferase. This enzyme has a 40% sequence similarity with *Fasciola hepatica*.

Succinyl CoA synthetase, alternatively referred to as Succinate-CoA ligase, has a pivotal function in the citric acid cycle, serving as one of the enzymes situated in the mitochondrial matrix. It catalyzes the reversible transformation between succinic-CoA and succinate, enabling the coupling of the formation of nucleoside triphosphate molecules (ATP or GTP) from nucleoside diphosphate molecules (ADP or PDB)[41,42)]. *Succinate CoA ligase* catalyzes the only substrate-level phosphorylation step in the tricarboxylic acid cycle[43–45)]. It suggests a kinetic reaction not commonly referred to as substrate synergism, where the presence of *Succinate CoA ligase* for one partial reaction stimulates another partial reaction[44)]. This is by the prediction of functions that have been performed using *PSIPRED* (Table 5.), namely, *Succinate CoA ligase* has a role including nucleoside binding, protein kinase activity, catalytic activity, and regulation of gene expression.

The outcomes of forecasting ammonia's impact on *cytochrome c nitrite reductase's* biological processes and molecular functions (Table 6) included various results such as the biosynthesis of large molecules, controlling gene expression, generating large molecules within cells, and processing of small molecules. One of the crucial steps in the biological nitrogen cycle is the reduction of six nitrite electrons to ammonia, which is catalyzed by the *cytochrome c nitrite reductase enzyme*. This enzyme participates in the anaerobic energy metabolism of ammonification of nitrate dissimilation[46)]. Nitrate reductase, which belongs to the sulfite oxidase family, is present in fungi and plants and plays a crucial role in assimilating nitrogen into the necessary cellular components such as amino acids and proteins. On the other hand, *nitrite reductase* (NiR) is an enzyme that catalyzes the reduction of nitrite (NO_2) to either *nitric oxide/nitrous monoxide* (NO/N_2O) or NH_3[47)]. Although studies on NiR bioelectrochemistry are not as common, some reports suggest that NiR is capable of electron transfer with electrodes, which provides an opportunity to investigate the enzyme turnover mechanism in more detail[48)]. In the *nitrate-to-ammonium reduction dissimilation pathway* (DNRA), *Cytochrome c nitrite reductase* (NrfA) is responsible for catalyzing the conversion of nitrite to ammonium, which competes with denitrification, thereby conserving nitrogen[49)]. One of the important pathways in DNRA is the dissimilatory reduction of nitrate to ammonia, which involves the conversion of nitrate to nitrite and then nitrite to ammonium. The second step in the DNRA pathway, which is the conversion of nitrite to ammonium, requires six electrons and eight protons, and is catalyzed by *cytochrome c nitrite reductase*[50)].

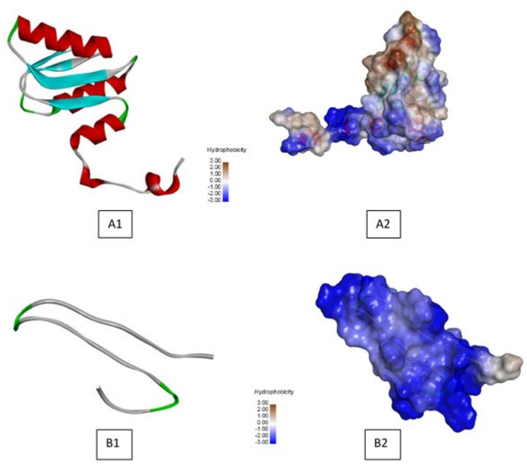

Fig 7. Structure drawings and 3D. A1) 3D structure of *Succinate CoA ligase*; A2) Physicochemical characteristics of *Succinate CoA ligase*; B1) Structure 3D *Ammonia form cytochrome c nitrite reductase*; B2) Physicochemical characteristics of *Ammonia form cytochrome c nitrite reductase*.

Table 4. Amino acid sequence of PPF *C. vulgaris*.

Sample	Amino Acid Sequence
ORF 1: Succinate CoA ligase	MQKDLFAMRDESQEDPREV AASKYDLNYIGLDGNIGCM VNGAGLAMATMDIIKLRGG APANFLDVGGNASEDQVVA AFKILTSDPQVKASQR
ORF2: Ammonia form cytochrome c nitrite reductase	MHGQWRWAGHGNHGHYQ VKGRRSSKFP

The following are the results of Biological Process Prediction based on GO analysis on PSIPRED (Table 5.)

Table 5. Results of biological process predictions based on GO analysis on PSIPRED.

GO term	Activities	Prob	SVM Reliability
0008104	protein localization	0.68	H
0009059	macromolecule biosynthetic process	0.654	H
0007017	microtubule-based process	0.638	H
0045333	cellular respiration	0.637	H
0010468	regulation of gene expression	0.625	H
0034613	cellular protein localization	0.613	H
0055114	oxidation-reduction process	0.61	H
0046907	intracellular transport	0.593	H
0034645	cellular macromolecule biosynthetic process	0.559	H
0007264	small GTPase mediated signal transduction	0.522	H
0035556	transcription, DNA-templated	0.512	H
0044281	small molecule metabolic process	0.504	H

Following are the results of Molecular Function Prediction based on GO analysis on PSIPRED (Table 6).

Table 6. Predicted results of molecular function based on GO analysis on PSIPRED.

GO term	Activities	Prob	SVM Reliability
0003824	catalytic activity	0.95	H
0001882	nucleoside binding	0.836	H
0017076	purine nucleotide binding	0.82	H
0000166	nucleotide binding	0.814	H
0016491	oxidoreductase activity	0.777	H
0035639	purine ribonu-cleoside triphos-phate binding	0.752	H
0003676	nucleic acid binding	0.748	H
0016818	hydrolase activity, acting on acid anhy-drides in phosphorus containing anhydrides	0.7	H
0005524	ATP binding	0.618	H
0003723	RNA binding	0.606	H
0004672	protein kinase activity	0.549	H
0016817	hydrolase activity, acting on acid anhydrides	0.52	H

Cellular component prediction results obtained the highest activity in the extracellular vesicular exosome, vesicle, and extracellular regions (Table 7). Extracellular Vesicular is a heterogeneous group of cell-derived membrane structures consisting of exosomes and microvesicles, each of which originates in the endosome system or is detached from the plasma membrane. Exosomes have been reported to be secreted by B lymphocytes, and dendritic cells with potential functions associated with immune regulation and are considered for use as a medium in antitumoural immune responses [51]. Extracellular vesicles play a critical role in regulating not only normal physiological processes, such as immune surveillance, stem cell maintenance, tissue repair, and blood clotting but also the pathologies that underlie certain diseases [52,53]. The following are the results of the Prediction of the Cellular Component based on GO analysis on *PSIPRED* (Table 7.).

Table 7. Prediction results of cellular components based on GO analysis on PSIPRED.

GO term	Activities	Prob	SVM Re-liability
0070062	extracellular vesicular exosome	0.925	H
0031982	vesicle	0.874	H
0005576	extracellular region	0.68	H
0016020	membrane	0.625	H
0031090	organelle membrane	0.62	H
0031988	membrane-bounded vesicle	0.583	H
0005739	mitochondrion	0.534	H
0000139	Golgi membrane	0.505	H

3.8 Protein Docking Analysis Results

The result of docking with rigid docking using *ClusPro* tools produces 26 different models with the lowest energy. The lowest energy produced is in cluster 4, with an energy of -923.8 (Table 8). However, the results of ClusPro can not be carried out by analyzing its protein interactions.

NNV Capsid Virus protein (NNCVP) is a structural protein that forms the outermost layer of the virion (Fig. 8). It plays a crucial role in viral morphogenesis and facilitates binding to hemoglobin and transferrin, leading to anemia in infected fish. NNV morphogenesis involves the participation of neural proteins that interact with NNCVP. *Viral nervous necrosis* can cause damage to the cerebellum, optic tectum, and retina in fish, and can be transmitted both horizontally and vertically[54]. The Stripped jack nervous necrosis virus, which replicates close to the swimbladder, causes necrosis and vacuolization of cells and tissues around the spinal cord. The virus can spread to the brain via the infected spinal cord, axonal transport, and the vagus nerves[55]. VNN can infect the host's body via endocytosis and macropinocytosis, accompanied by an increase in sialic acid on the surface of the host cell. It can bind to HSC70 (Heat Shock Cognate protein 70), which has been identified as a receptor or co-receptor for the NNV virus that infects grouper. The capsid protein of NNV is utilized to initiate the infection by binding to this protein.

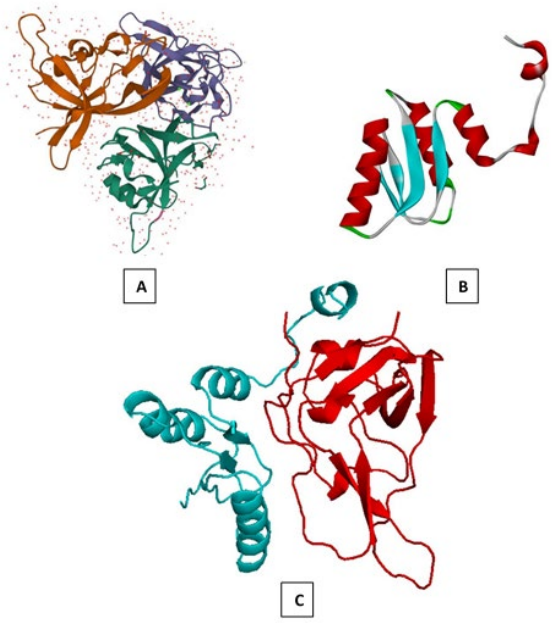

Fig 8. Protein docking results. (A). The capsid protein of Grouper nervous necrosis virus has a truncated P-domain, and its crystal structure has been determined at a resolution of 1.2A (ID 4RFU); (b). Structure of *Succinate CoA ligase*; (C). Results of protein capsid protein (red) and *Succinate CoA ligase* (blue) docking with ClusPro.

Table 8. Protein capsid protein and *Succinate CoA ligase* docking scores with ClusPro.

Cluster	Members	Representative	Weighted Score
0	121	Center	-678.3
		Lowest Energy	-840.6
1	121	Center	-740.2
		Lowest Energy	-907.7
2	82	Center	-793
		Lowest Energy	-895.8
3	79	Center	-858.5
		Lowest Energy	-873.6
4	57	Center	-753.3
		Lowest Energy	-923.8
5	45	Center	-710.3
		Lowest Energy	-799.4
6	42	Center	-699.4
		Lowest Energy	-764.5
7	41	Center	-716.9
		Lowest Energy	-723.3
8	35	Center	-717.9
		Lowest Energy	-778.7
9	30	Center	-673.2
		Lowest Energy	-739.7
10	29	Center	-677.9
		Lowest Energy	-872.3
11	29	Center	-710.9
		Lowest Energy	-750.8
12	29	Center	-742.4
		Lowest Energy	-800.1
13	28	Center	-711.8
		Lowest Energy	-826
14	23	Center	-728.4
		Lowest Energy	-828.4
15	21	Center	-700.6
		Lowest Energy	-719.7
16	19	Center	-690.4
		Lowest Energy	-744.5
17	18	Center	-752.4
		Lowest Energy	-752.4
18	17	Center	-684.8
		Lowest Energy	-827.8
19	16	Center	-708.8
		Lowest Energy	-757.1
20	14	Center	-694.3
		Lowest Energy	-765.1
21	13	Center	-701.8
		Lowest Energy	-732.7
22	12	Center	-681.9
		Lowest Energy	-719.6
23	10	Center	-734.3
		Lowest Energy	-734.3
24	8	Center	-675
		Lowest Energy	-733.3
25	6	Center	-722.2
		Lowest Energy	-722.2
26	5	Center	-699.7
		Lowest Energy	-735

Furthermore, the results with flexible docking using Haddock showed an interaction of -15.8 +/-13.2 (Fig. 9, Table 8), showing the best results on the 4th cluster with a value of Center of -753.3, and Lowest Energy -923.8. The amino acid interactions involved have been detected between the two proteins (Fig. 10).

The modeling results indicate that there are amino acid interactions between succinate and capsid proteins, which are the protein shells that encase the viral genome and are typically composed of multiple amino acids that can interact with other molecules, including succinate. It is possible that succinate could interact with certain amino acids within the capsid protein through hydrogen bonding, electrostatic interactions, or other chemical interactions. Furthermore, Guilon *et al*. (2022) reported that succinate can disrupt the virus replication cycle through a succinylation mechanism[56)]

Fig. 9. The result of docking capsid protein (red) and *Succinate CoA ligase* (blue) with Haddock

4. CONCLUSION

The Pigment-Protein Fraction (PPF) in *C. vulgaris* was successfully identified with a protein molecular weight of 14 kDa and 35 kDa and a base pair sequence length of 313 bp. PPF contains 2.19 - 4.02 x 10^{-13} mg/cell of protein and 3.62 - 4.98 x 10^{-09} mg/cell of fat. The results of matching the PPF gene sequences discovered with the results available in GenBank show similarities in the PPF gene sequences, and they still have phylogenetic relationships, as shown in the phylogenetic tree. Based on physicochemical properties and biological processes, molecular functions, and cellular components found in succinate ligase proteins, the structure and interaction of succinate ligase protein and VNN virus capsid were modeled, and the amino acid interactions involved between the two proteins have been detected. In the future, it will be possible to characterize proteins in *Chlorella* thoroughly to determine the most effective interaction with the VNN virus capsid, allowing it to be recommended as a VNN antiviral agent.

Acknowledgment

A great appreciation was delivered to Institute for Research and Community Service (LPPM) Universitas Brawijaya, which Financed the Indonesian Collaborative Research (RKI) in 2022 under Research Contract Number: 1073.2 / UN10. C10/TU/2022, dated May 12, 2022.

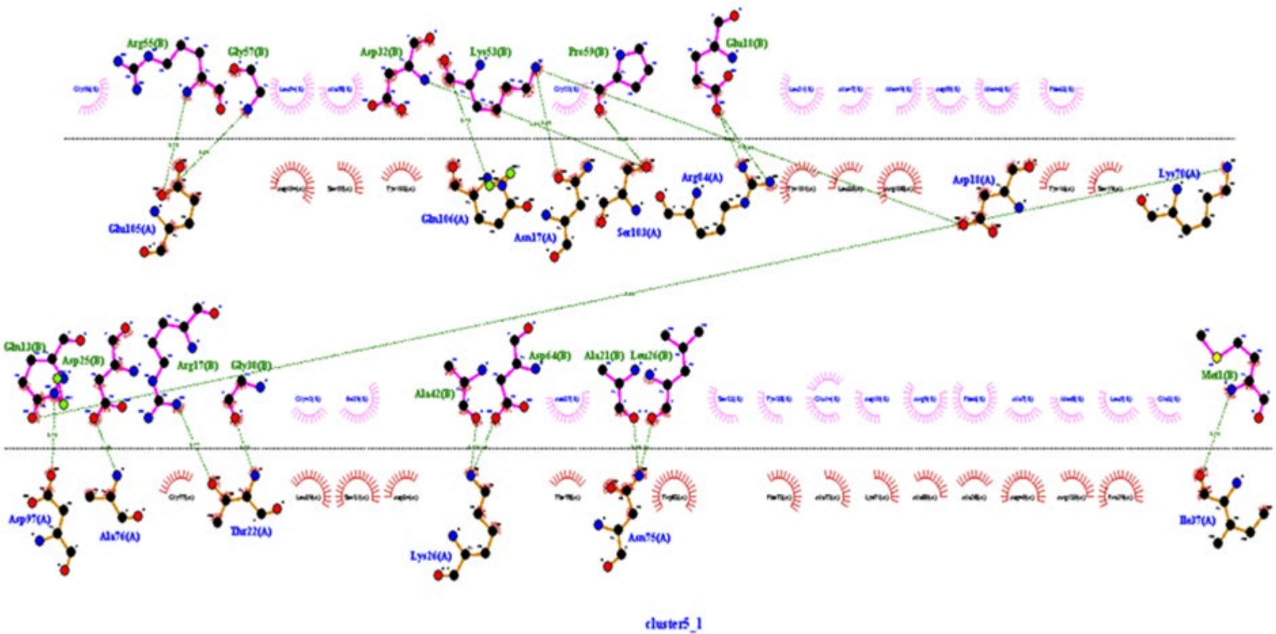

Fig. 10. Amino acid interaction between *Succinate CoA ligase* and Capsid protein

References

1) M.T. Ahmad, M. Shariff, F. Md. Yusoff, Y.M. Goh, and S. Banerjee, "Applications of microalga *chlorella vulgaris* in aquaculture," *Rev. Aquac.*, 12 (*1*) 328–346 (2020).
2) A. Saberi, M.J. Zorriehzahra, H. Emadi, S. Kakoolaki, and S.M.R. Fatemi, "Effects of chlorella *vulgaris* on blood and immunological parameters of caspian sea salmon (*salmo trutta caspius*) fry exposed to viral nervous necrosis (vnn) virus," *Iran. J. Fish. Sci.*, 16 (*2*) 494–510 (2017).
3) U. Yanuhar, D. Arfiati, M. Musa, N.S. Junirahma, and N.R. Caesar, "The Status of VNN (*Viral Nervous Necrosis*)-lnfected Grouper Fish Tissue with *Chlorella vulgaris* Extract as Anti-Virus Candidate," in: J. Phys. Conf. Ser., IOP Publishing, 2020: p. 12036.
4) U. Yanuhar, "Mikroalga Laut *Nannochloropsis oculata*," I, UB Press, Malang, 2016. https://books.google.co.id/books?id=EUpNDwAAQBAJ&printsec=frontcover&hl=id&source=gbs_ge_summary_r&cad=0#v=onepage&q&f=false.
5) M.I. Rizaldi, A. Rahman, and N.B. Prihantini, "Effect of bubble size on the growth of synechococcus hs-9 microalgae with double loop fluid oscillator," *EVERGEEN Joint Journal of Novel Carbon resource Science Green Asia Strategy.*, 8 (*4*) 866–871 (2021) doi.org/10.5109/4742134.
6) N.B. Prihantini, N. Rakhmayanti, S. Handayani, W. Sjamsuridzal, and W. Wardhana, "Biomass production of indonesian indigenous leptolyngbya strain on npk fertilizer medium and its potential as a source of biofuel," *EVERGEEN Joint Journal of Novel Carbon resource Science Green Asia Strategy.*, 7 (*4*) 593–601 (2020) doi.org/10.5109/4150512.
7) A. Mufidah, A. Agustono, S. Sudarno, and D.D. Nindarwi, "Teknik kultur *Chlorella* sp. skala laboratorium dan intermediet di balai perikanan budidaya air payau (BPBAP) situbondo jawa timur," *J. Aquac. Fish Heal.*, 7 (*2*) 50–56 (2018).
8) J.D. Putra, A. Rahman, and N.B. Prihantini, "Bubble coalescence on photobioreactor bubble columns by using horizontal baffle for microalgae," *EVERGEEN Joint Journal of Novel Carbon resource Science Green Asia Strategy.*, 8 (*4*) 861–865 (2021) doi.org/10.5109/4742133.
9) C. Safi, B. Zebib, O. Merah, P.-Y. Pontalier, and C. Vaca-Garcia, "Morphology, composition, production, processing and applications of *Chlorella vulgaris*: a review," *Renew. Sustain. Energy Rev.*, 35 265–278 (2014). doi:10.1016/J.RSER.2014.04.007.
10) U. Yanuhar *et al.*, "Influence of a pigment protein fraction from chlorella *vulgaris* isolated in indonesia on *β-actin* and MHC-1 response to viral infected humpback grouper," *Syst. Rev. Pharm.*, 11 (*7*) 352–362 (2020).
11) Z. Nurachman *et al.*, "Tropical marine chlorella sp. pp1 as a source of photosynthetic pigments for dye-sensitized solar cells," *Algal Res.*, 10 25–32 (2015).
12) S. Joshi, R. Kumari, and V.N. Upasani, "Applications of algae in cosmetics: an overview," *Int. J. Innov. Res. Sci. Eng. Technol*, 7 (*2*) 1269 (2018).
13) U. Yanuhar, M. Musa, D. Arfiati, N.R. Caesar, and N.S. Junirahma, "In-vivo Test of Chlorella Protein Fragments as Nucleotide Vaccine Candidates in Grouper *Viral Nervous Necrosis* (VNN) Infection against Haematological Response," in: 6th ICAMBBE (International Conf. Adv. Mol. Biosci. Biomed. Eng. 2019, SCITEPRESS – Science and Technology Publications, 2020: pp. 79–83. doi:10.5220/0009588100790083.
14) U. Yanuhar, and A. Khumaidi, "The application of pigment-protein fraction from nannochloropsis oculata on β-actin response of *Cromileptes altivelis* infected with *viral nervous necrosis*," *J. Akuakultur Indones.*, 16 (*1*) 22 (2017). doi:10.19027/jai.16.1.22-32.
15) G.M. Morris, and M. Lim-Wilby, "Molecular docking," *Mol. Model. Proteins*, 365–382 (2008).
16) V. Salmaso, and S. Moro, "Bridging molecular docking to molecular dynamics in exploring ligand-protein recognition process: an overview," *Front. Pharmacol.*, 9 923 (2018).
17) I. Jomaa *et al.*, "Experimental, computational, and in silico analysis of (c8h14n2) 2 [cdcl6] compound," *J. Mol. Struct.*, 1213 128186 (2020).
18) U. Yanuhar, N.R. Caesar, and M. Musa, "Identification of local isolate of microalgae *Chlorella vulgaris* using ribulose-1, 5-bisphosphate carboxylase/oxygenase large subunit (rbcL) gene," in: IOP Conf. Ser. Mater. Sci. Eng., IOP Publishing, 2019: p. 22038.
19) G. Gärtner *et al.*, "Microscopic investigations (lm, tem and sem) and identification of chlorella isolate r-06/2 from extreme habitat in bulgaria with a strong biological activity and resistance to environmental stress factors," *Biotechnol. Biotechnol. Equip.*, 29 (*3*) 536–540 (2015).
20) M. Saha, and P.K. Bandyopadhyay, "Phytochemical screening for identification of bioactive compound and antiprotozoan activity of fresh garlic bulb over trichodinid ciliates affecting ornamental goldfish," *Aquaculture*, 473 181–190 (2017).
21) Association of Official Analytical Chemists (AOAC), "Official Methods of Analysis of Association of Official Analytical Chemists," 18th Editi, AOAC International Gaithrsburg, Washington, DC., 2005. http://www.scribd.com/doc/131064441/AOAC-2005.
22) S.R. Ardiansyah, A.M. Orlando, A. Rahman, and N.B. Prihantini, "Tubular photobioreactor: a preliminary experiment using synechococcus sp.(cyanobacteria) cultivated in npk media for biomass production as biofuel feedstock," *EVERGEEN Joint Journal of Novel Carbon resource Science Green Asia Strategy.*, 6 (*2*) 157–161 (2019) doi.org/10.5109/2321011.

23) V.M. Weis, E.A. Verde, and W.S. Reynolds, "Characterization of a short form peridinin-chlorophyll-protein (pcp) cdna and protein from the symbiotic dinoflagellate S*ymbiodinium muscatinei* (dinophyceae) from the sea anemone *Anthopleura elegantissima* (cnidaria) 1," *J. Phycol.*, 38 (*1*) 157–163 (2002).
24) M. Kawaroe, T. Prartono, and G. Saefurahman, "Kepadatan dan laju pertumbuhan spesifik *Nannochloropsis* sp. pada kultivasi heterotropik menggunakan media hidrolisat singkong," *Omni-Akuatika*, 11 (*2*) (2015).
25) T. Novianti, "Kandungan betakaroten kultur mikroalga (chlorella *vulgaris*) dengan perbedaan sumber cahaya dan kepadatan awal inokulum (kai)," *Mangifera Edu*, 4 (*1*) 46–61 (2019).
26) I. Putra, A.A.M.D. Anggreni, and I.W. Arnanta, "Pengaruh jenis media terhadap konsentrasi biomassa dan klorofil mikroalga *Tetrselmis chuii*," *J. Rekayasa Dan Manaj. Agroindustri*, 3 (*2*) 1–7 (2015).
27) D.E. Satriaji, M. Zainuri, and I. Widowati, "Study of growth and n, p content of microalgae *Chlorella vulgaris* cultivated in different culture media and light intensity," *J. Teknol.*, 78 (*4–2*) (2016).
28) A. Sukoyo, G. Djoyowasito, and Y. Wibisono, "Sintesis karbon aktif berbahan dasar mikroalga *Chlorella vulgaris* menggunakan aktivator koh dan iradiasi gelombang mikro," *Rekayasa Mesin*, 10 (*2*) 121–129 (2019).
29) J. Jiang *et al.*, "Characterization of the peridinin–chlorophyll a-protein complex in the dinoflagellate symbiodinium," *Biochim. Biophys. Acta (BBA)-Bioenergetics*, 1817 (*7*) 983–989 (2012).
30) J. Ringo, G. Sharon, and D. Segal, "Bacteria-induced sexual isolation in drosophila," *Fly (Austin).*, 5 (*4*) 310–315 (2011).
31) H.S. Bahar, A. Djunaedi, and W. Widianingsih, "Perbedaan lama fotoperiode terhadap total lipid kultur mikroalga *Chlorella vulgaris*," *J. Mar. Res.*, 11 (*1*) 92–97 (2022).
32) A.M. Orlando, W. Sjamsuridzal, W. Wardhana, and N.B. Prihantini, "Biomass production and lipid content of leptolyngbya hs-16 grown in bubble column photobioreactors (bcpbr) with air bubbler pore variation," *EVERGEEN Joint Journal of Novel Carbon resource Science Green Asia Strategy.*, 8 (*4*) 885–889 (2021) doi.org/10.5109/4742137.
33) L.M.Z. Ash-Shalehah, C. Anggraeni, and E. Gloria, "Development of microalgae-microbial fuel cell (mmfc) technology using microalgae consortium of *chlorella* vulgaris and spirulina platensis," *EVERGEEN Joint Journal of Novel Carbon resource Science Green Asia Strategy.*, 9 (*2*) 476–483 (2022) doi.org/10.5109/4794175.
34) A. Rahman, and N.B. Prihantini, "Biomass production and synthesis of biodiesel from microalgae synechococcus hs-9 (cyanobacteria) cultivated using bubble column photobioreactors," *EVERGEEN Joint Journal of Novel Carbon resource Science Green Asia Strategy.*, 7 (*4*) 564–570 (2020) doi.org/10.5109/4150507.
35) X. Liu, Y. Hong, Y. He, and Y. Liu, "Growth and high-valued products accumulation characteristics of microalgae in saline-alkali leachate from inner mongolia," *Environ. Sci. Pollut. Res.*, 26 36985–36992 (2019).
36) Y. V Maleeva, K. V Neverov, Y.N. Obukhov, and M.S. Kritsky, "Water soluble chlorophyll-binding proteins of plants: structure, properties and functions," *Mol. Biol.*, 53 876–888 (2019).
37) K.M. Supasri *et al.*, "Characterisation and bioactivity analysis of peridinin-chlorophyll a-protein (pcp) isolated from *Symbiodinium tridacnidorum* cs-73," *J. Mar. Sci. Eng.*, 9 (*12*) 1387 (2021).
38) B.G. Hall, "Building phylogenetic trees from molecular data with mega," *Mol. Biol. Evol.*, 30 (*5*) 1229–1235 (2013). doi:10.1093/molbev/mst012.
39) W. Yang, C. Catalanotti, T.M. Wittkopp, M.C. Posewitz, and A.R. Grossman, "Algae after dark: mechanisms to cope with anoxic/hypoxic conditions," *Plant J.*, 82 (*3*) 481–503 (2015).
40) A. Atteia, R. van Lis, A.G.M. Tielens, and W.F. Martin, "Anaerobic energy metabolism in unicellular photosynthetic eukaryotes," *Biochim. Biophys. Acta (BBA)-Bioenergetics*, 1827 (*2*) 210–223 (2013).
41) T.-Y. Feng *et al.*, "Examination of metabolic responses to phosphorus limitation via proteomic analyses in the marine diatom *Phaeodactylum tricornutum*," *Sci. Rep.*, 5 (*1*) 10373 (2015).
42) G. Kacso *et al.*, "Two transgenic mouse models for β-subunit components of succinate-coa ligase yielding pleiotropic metabolic alterations," *Biochem. J.*, 473 (*20*) 3463–3485 (2016).
43) M.E. Fraser, K. Hayakawa, M.S. Hume, D.G. Ryan, and E.R. Brownie, "Interactions of gtp with the atp-grasp domain of gtp-specific succinyl-coa synthetase," *J. Biol. Chem.*, 281 (*16*) 11058–11065 (2006).
44) X. Sun *et al.*, "Succinate coenzyme a ligase beta-like protein from *Trichinella spiralis* suppresses the immune functions of rat pbmcs in vitro and inhibits the secretions of interleukin-17 in vivo," *Vaccines*, 7 (*4*) 167 (2019).
45) J. Huang, and M.E. Fraser, "Structural basis for the binding of succinate to succinyl-coa synthetase," *Acta Crystallogr. Sect. D Struct. Biol.*, 72 (*8*) 912–921 (2016).
46) S. Shahid, M. Ali, D. Legaspi-Humiston, J. Wilcoxen, and A.A. Pacheco, "A kinetic investigation of the early steps in cytochrome c nitrite reductase (ccnir)-catalyzed reduction of nitrite," *Biochemistry*, 60 (*26*) 2098–2115 (2021).
47) M. Ali *et al.*, "Trapping of a putative intermediate in the *cytochrome c nitrite reductase* (ccnir)-catalyzed reduction of nitrite: implications for the ccnir reaction

mechanism," *J. Am. Chem. Soc.*, 141 (*34*) 13358–13371 (2019).

48) R.D. Milton, and S.D. Minteer, "Enzymatic bioelectrosynthetic ammonia production: recent electrochemistry of nitrogenase, nitrate reductase, and nitrite reductase," *Chempluschem*, 82 (*4*) 513–521 (2017).

49) D. Bykov, and F. Neese, "Six-electron reduction of nitrite to *ammonia by cytochrome c nitrite reductase*: insights from density functional theory studies," *Inorg. Chem.*, **54** (*19*) 9303–9316 (2015).

50) J. Campeciño *et al.*, "*Cytochrome c nitrite reductase* from the bacterium geobacter lovleyi represents a new nrfa subclass," *J. Biol. Chem.*, **295** (*33*) 11455–11465 (2020).

51) G. Van Niel, G. d'Angelo, and G. Raposo, "Shedding light on the cell biology of extracellular vesicles," *Nat. Rev. Mol. Cell Biol.*, **19** (*4*) 213–228 (2018).

52) M. Yáñez-Mó *et al.*, "Biological properties of extracellular vesicles and their physiological functions," *J. Extracell. Vesicles*, **4** (*1*) 27066 (2015)

53) M. Zarà *et al.*, "Biology and role of extracellular vesicles (evs) in the pathogenesis of thrombosis," *Int. J. Mol. Sci.*, **20** (*11*) 2840 (2019).

54) P.-Y. Huang *et al.*, "Screening for the proteins that can interact with grouper nervous necrosis virus capsid protein," *Viruses*, **12** (*9*) 985 (2020).

55) J.Z. Costa, and K.D. Thompson, "Understanding the interaction between betanodavirus and its host for the development of prophylactic measures for viral encephalopathy and retinopathy," *Fish Shellfish Immunol.*, **53** 35–49 (2016). doi:10.1016/j.fsi.2016.03.033.

56) A. Guillon *et al.*, "Host succinate inhibits influenza virus infection through succinylation and nuclear retention of the viral nucleoprotein," *EMBO J.*, **41** (*12*) e108306 (2022).

Appendix 1. PPF phylogenetics from *C. vulgaris* was compared with GenBank data